Sensors and Materials, Vol. 32, No. 1 (2020) 357–373
MYU Tokyo

S & M 2107

Curve Fitting Approach for Fundamental Frequency Measurement for Power Systems

Chih-Hung Lee,[1*] Chi-Chun Huang,[2] and Men-Shen Tsai[2,3]

[1]Graduate Institute of Mechanical and Electrical Engineering, National Taipei University of Technology, 1, Sec. 3, Zhong-xiao E. Rd., Taipei 10608, Taiwan
[2]Graduate Institute of Automation Technology, National Taipei University of Technology, 1, Sec. 3, Zhong-xiao E. Rd., Taipei 10608, Taiwan
[3]Research Center of Energy Conservation for New Generation of Residential, Commercial, and Industrial Sectors, National Taipei University of Technology, 1, Sec. 3, Zhong-xiao E. Rd., Taipei 10608, Taiwan

(Received January 19, 2019; accepted December 13, 2019)

Keywords: power quality, curve fitting, frequency measurement

In recent years, owing to an increase in electrical energy consumption, the quality and safety issues of power systems have drawn considerable attention. The frequency of a power system is an important indicator of its stability. The system frequency will drop when large generator sets are tripped. Therefore, it is important to measure the fundamental frequency of a power system accurately. The power system frequency can be estimated through various methods in time or frequency domains. Among these methods, curve fitting is a time domain approach that can be used to identify the parameters of a model using the input information obtained by utilizing a nonlinear regression method to fit the input curve. The physical phenomenon of a power system is described by a mathematical model. The curve fitting approach is applied to find the parameters such that the model is closer to the measured signal. These parameters are used to obtain the fundamental frequency of the power system. In this paper, the genetic algorithm (GA) is compared with the conventional regression analysis (RA) method for identifying the parameters of the model. The performance of curve fitting using different mathematical models on various power system events is discussed.

1. Introduction

In recent years, owing to the rising environmental awareness, many countries around the world are now developing green renewable energy using conventional power generation technologies to prevent environmental pollution. Various industries, such as conventional, semiconductor, chemical, and software industries, have been developed rapidly over the past decades. As a result, power consumption has increased rapidly. During a typical operation, generators may be tripped owing to an accident. The power generation and load cannot be balanced. This incident causes a rapid decline in system frequency. The dropping of the system frequency may further cause the tripping of other generation units. The chain reaction may

*Corresponding author: e-mail: t100669021@ntut.edu.tw
https://doi.org/10.18494/SAM.2020.2594

ISSN 0914-4935

result in power system black out. To alleviate the problem, a load shedding scheme is needed by installing low-frequency relays in systems. Accurately measuring the frequency of a power system is important for evaluating the stability of the system.[1–6] At present, many techniques have been proposed for measuring the power system frequency. Common techniques include frequency domain interpolation, Prony's method,[7,8] the zero crossing method,[9,10] discrete Fourier transform (DFT) or fast Fourier transform (FFT),[1,3,6] and so on. In this study, the curve fitting approach is utilized. Curve fitting can be used to calculate the frequency in the absence of some sampling points. The missing sampling points can be obtained by the interpolation approach. On the other hand, the genetic algorithm (GA) is used to estimate a parameter directly. Two different mathematical models are investigated in this study to compare their performance characteristics. The first model considers only the ideal power signal form. The frequency variation term is used in addition to the ideal power signal for the second model. The performance characteristics of the two models are compared under various scenarios.

2. Materials and Methods

Traditionally, the ideal power signal is regarded as a sine wave, which is mainly composed of three parts, namely, amplitude, frequency, and phase. In this study, the curve fitting method is used to estimate the power system frequency in accordance with IEEE1459-2000.[11] In addition to the stationary frequency model, the frequency variation term is also considered.[12]

2.1 Basic power signal definition

The traditional power system signal is described in IEEE1459-2000.[11] The voltage signal can be expressed as

$$v(t) = \sqrt{2V}\sin(2\pi ft + \theta_v)\ . \tag{1}$$

If an ideal linear load is connected, the current signal can be expressed as

$$i(t) = \sqrt{2I}\sin(2\pi ft + \theta_i)\ , \tag{2}$$

where V is the voltage root mean square (RMS), I is the current RMS, f is the signal frequency, θ_v and θ_i are the voltage and current phase angles, respectively, and t is the time.

When a voltage is applied to a nonlinear load, the linear relationship between voltage and current does not apply. Nonlinearity causes waveform distortion, resulting in the current waveform no longer being a pure sinusoidal waveform. This phenomenon is called harmonic distortion. Therefore, for voltage and current signals containing harmonic components, it can be expressed mathematically as[13]

$$v(t) = \sum_{k=1}^{\infty} V_k \sin(2\pi f_k t + \theta_k), \tag{3}$$

$$i(t) = \sum_{k=1}^{\infty} I_k \sin(2\pi f_k t + \psi_k), \tag{4}$$

where V_k is the kth order of the voltage harmonic amplitude, I_k is the kth order of the current harmonic amplitude, f_k is the kth harmonic frequency of the input signal, k is the kth harmonic order, and θ_k and ψ_k are the initial phase angles of the voltage and current signals, respectively.

2.2 Noise

In the process of signal transmission, the signal will be interfered by some external energy, e.g., noise. Noise will cause signal distortion. The noise source may be generated by the receiving system in addition to the power system.

There are many types of noise. The analog noise used in this study is white noise, also known as Gaussian noise. White noise is a random signal with a constant power spectral density, that is, the power of this signal is the same in each frequency band, and its expected value is zero. The mathematical expression is shown as

$$E\{W\} = 0, \tag{5}$$

where E is the expected value and W is the random vector.

2.3 Data fitting and regression analysis (RA)

Curve fitting is a method that derives the parameters of a mathematical model for approximating the input and output of the data. To utilize the curve fitting method for identifying the power system fundamental frequency, a power system signal model is required. Conventionally, RA is applied to identify the parameters of a given model.

2.4 Power system signal model of curve fitting

For AC signals, when the frequency of the power system changes, the stationary power signal model cannot be used to describe the characteristics of the power system signal since the signal is not periodic. In this study, the sinusoidal function is used to represent the power system signal, i.e., voltage. The parameters are the amplitude A_m, frequency ω, phase φ, and rate of change of frequency (ROCOF). The general sinusoidal signal that represents an AC power system analysis is defined on the basis of IEEE Standard C37.118.2 as[13]

$$x(t) = A_m \cos(\omega t + \varphi). \tag{6}$$

The sinusoidal signal can be expressed as

$$x(t) = A_m \cos\Phi, \tag{7}$$

where A_m is the amplitude and Φ is the angle vector. The frequency function can be defined as

$$f(t) = \frac{1}{2\pi}\frac{d\Phi(t)}{dt}. \tag{8}$$

ROCOF is defined as

$$ROCOF(t) = \frac{df(t)}{dt}. \tag{9}$$

From Eqs. (6) and (9), if the frequency is changed at a fixed rate, the phasor equation can be rewritten as[12,14,15]

$$x(t) = A_m \cos\left[\left(\omega + \frac{f_c}{2}t\right)t + \varphi\right], \tag{10}$$

where f_c is the ROCOF.

2.5 RA

In the conventional curve fitting approach, RA is applied to identify the parameters. The signal frequency of the power system model is considered nonlinear; therefore, a nonlinear regression approach is applied.

According to Eqs. (6) and (10), the power system frequency signal model can be described as

$$Y \approx f(X), \tag{11}$$

where Y is the power system signal vector and $f(X)$ is the mathematic model. X is the parameter vector of the power system signal model. In general, Y is not equal to $f(X)$. Thus, an iterative approach is required to find the optimal parameters by minimizing the sum of squared error (SSE) defined as

$$SSE = \sum_{i=1}^{m}\left[y_i - f(x_i, X)\right]^2, \tag{12}$$

where y_i is the element of the power system signal, x_i is the fitting output, X is the parameter vector of the power system signal model, i is the ith sampled point of the power system signal,

and m is the total number of sampled data. The gradient descent approach can be used to find the minimum SSE. The gradient descent equation can be written as

$$SSE^{(t+1)} = SSE^{(t)} - \gamma \nabla f(SSE^{(t)}), \tag{13}$$

where t is the number of iterations, γ is the learning rate, and ∇ is the gradient operator. An iteration is terminated when the SSE is converged. Otherwise, another iteration of the fitting procedure is performed.

2.6 GA

Although the parameters used in models described in Eqs. (6) and (10) can be obtained by RA, they can also be identified by applying GA. GA is a metaheuristic method developed based on the Darwin's theory of natural selection.[16–18] By removing weak creatures and retaining more adaptive organisms, the most powerful creatures can be obtained eventually.

2.6.1 Chromosome representation

The variables used in the power system frequency model are encoded in GA as genes in chromosomes. In this paper, amplitude, frequency, frequency variation, harmonic amplitude, and noise are the variables that must be determined. Two approaches in GA, namely, real number encoding and binary encoding, can be applied to encode these variables. In binary encoding, variables are encoded in binary string forms. The longer the binary string, the higher the accuracy. However, a longer execution time is required for longer binary strings. Since the time to obtain these parameters is critical, the binary string encoding approach is not used. For the real number encoding approach, each parameter is represented by a real number. Since the real number is both a solution and a gene representation, no decoding procedure is required. Compared with those of binary coding, the calculation time of real number encoding can be greatly shortened and its calculation accuracy can be increased if a double precision representation is used.

2.6.2 Population

When generating chromosomes, restriction on the parameters must be considered. For example, when the nominal frequency of a power system is 60 Hz, a reasonable range of 55–65 Hz is used. The gene that represents the frequency parameter in chromosomes will have a value between 55 and 65 Hz. The remaining variables, such as amplitude, phase, frequency variation, harmonic amplitude, and noise, are randomly generated in the given range as well. It is critical to determine the variable range. On one hand, it is desired that the searching space can be as large as possible. On the other hand, the calculation time of the algorithm is greatly increased when the search space is increased. A larger search space may also lead to an incorrect solution.

2.6.3 Fitness

Adaptability is an important indicator for determining the fitness of chromosomes. The fitness function is a method used to describe the performance of a chromosome. The fitness function is usually derived from experience or observation. When chromosomes are generated, the fitness function is used to evaluate them. Generally, the higher the fitness of a chromosome, the higher the quality of the chromosome. However, if the fitness of a chromosome is much higher than those of other chromosomes, it is very likely that the chromosome will dominate the evolutionary process and converge to an undesired solution. According to Eq. (12), the fitness function used in this study is expressed as

$$Fitness = \frac{1}{SSE}. \tag{14}$$

2.6.4 Crossover

Crossover is a natural biological behavior. By mating, the gene pool can be exchanged between individuals in a population. Different crossover strategies will result in different performance characteristics during the evolutionary process. Note that crossover does not guarantee that a higher quality chromosome is produced.

2.6.5 Mutation

Mutation is another natural biological behavior. During the evolutionary process, the allele of a gene may change owing to some external stimulation. The mutation process during GA is designed to prevent convergence to a local region, which is not a good solution for the problem.

2.6.6 Selection

In reality, individuals with a lower survivability will be eliminated. GA also embeds such a behavior. The algorithm relies on the fitness to evaluate each chromosome. Fitness is similar to the ability of organisms in nature to adapt to the environment. During the selection procedure, a chromosome with a higher fitness has a higher probability to be selected for the next generation.

2.7 Simulation process

The mathematical models to be used are Eqs. (6) and (10). The variable range is selected as follows: amplitude = [0.8, 1.2], frequency = [58, 61], phase = [$-\pi$, π], and ROCOF = [−5, 5]. A reasonable range of variables can avoid the divergence of RA and GA. The measured window length will determine the characteristics of the curve fitting process. When the window length is small, the calculation time will be reduced. However, a shorter window makes the fitting

result difficult to converge and probably cannot find the best solution. When the window length is very large, the probability of successful fitting increases and the residual value can be reduced. However, the frequency tracking ability decreases and the calculation time increases greatly when a longer window is used. Generally, the window length is between 8 and 12 cycles. The IEC 61000-4-7 standard has recommended the 5 Hz frequency resolution on the basis of the DFT technique. That is, the analysis information with a time length of 0.2 s is applied to harmonic and interharmonic analyses. Therefore, 12 cycles are used in this study. After the parameter ranges and window length are determined, RA and GA are applied to find the model parameters such that the model is closest to the input signal. The system frequency can be calculated using the parameters obtained. For each window, a set of model parameters is averaged by executing RA and GA several times.

3. Simulation Results

Four different power events are considered. Equations (6) and (10) are used to represent the power system frequency models. RA and GA are applied to identify the parameters of the curve fitting method. The results are represented graphically. The flow charts are shown in Figs. 1 and 2.

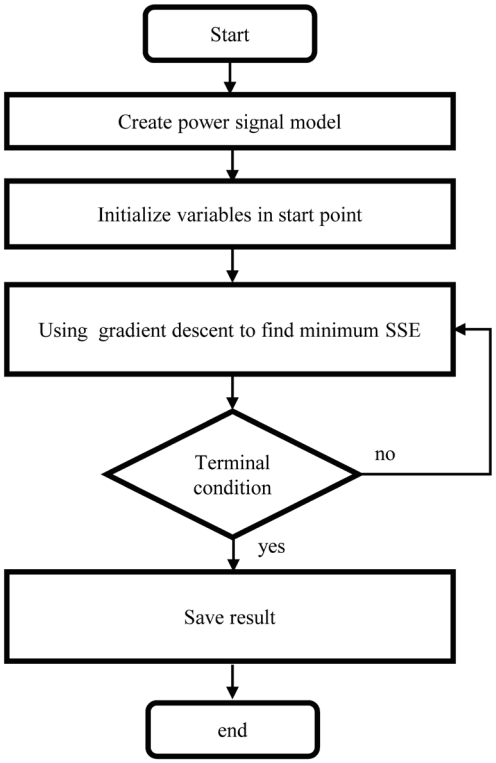

Fig. 1. Flowchart of RA.

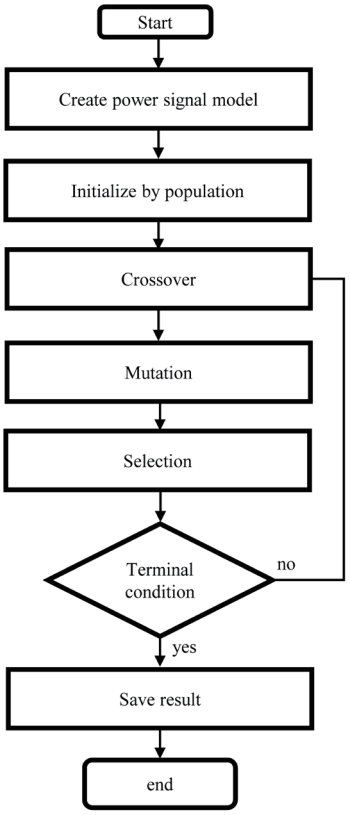

Fig. 2. Flowchart of GA.

3.1 Standard power signal measurement

In this case, the sampling frequency is 960 Hz, the window length is 12 cycles, and the simulation time is 0.2094 s. Equation (15) is used to represent the input signal.

$$x(t) = \cos\left(2\pi ft + \frac{\pi}{6}\right). \tag{15}$$

In Eq. (15), f is the fundamental frequency and t is the time. The frequency range is set to 58.5–60.5 Hz. The results are shown in Figs. 3 and 4 for the fundamental frequency of 59.8 Hz. The root-mean-square errors (RMSEs)[19,20] for both models are shown in Tables 1–4 with different frequencies.

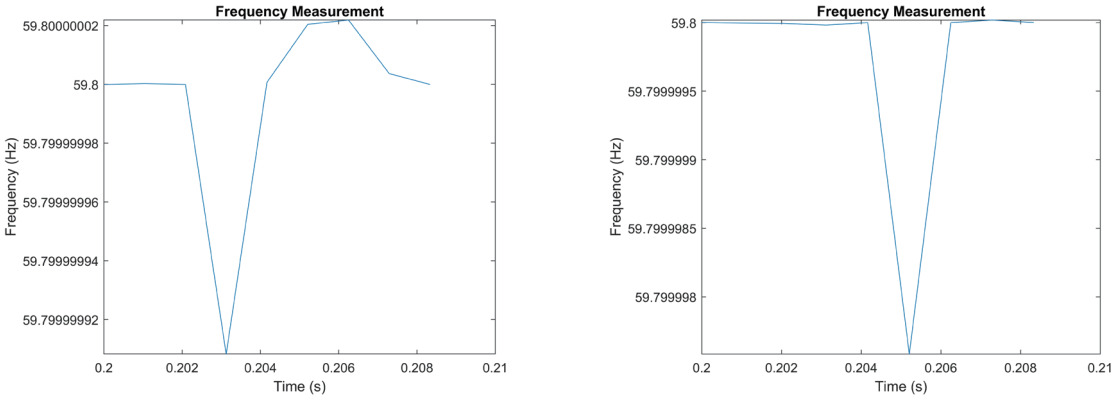

(a) (b)

Fig. 3. (Color online) Results obtained using (a) Eq. (6) and RA, and (b) Eq. (10) and RA.

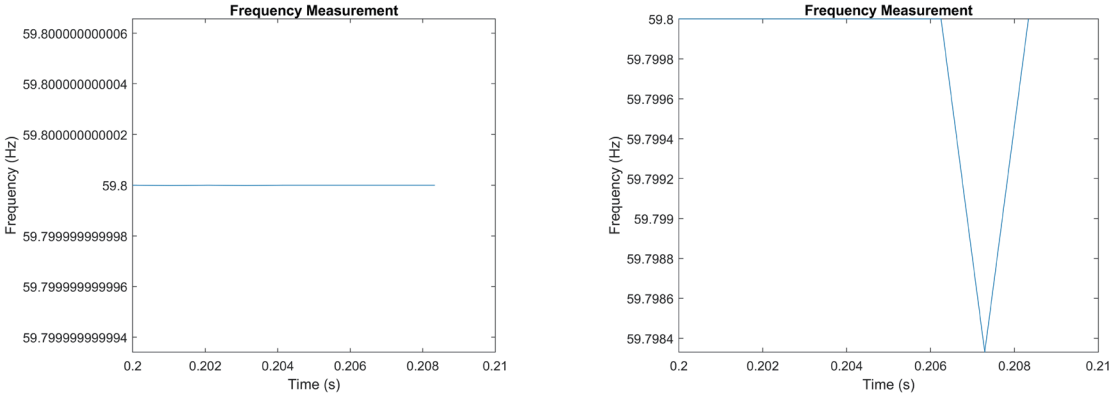

(a) (b)

Fig. 4. (Color online) Results obtained using (a) Eq. (6) and GA, and (b) Eq. (10) and GA.

Table 1
RMSEs of standard power signal [Eq. (6) and RA].

f (Hz)	RMSE (Hz)	f (Hz)	RMSE (Hz)	f (Hz)	RMSE (Hz)
58.5	2.17E−08	59.2	6.09E−06	59.9	7.75E−09
58.6	1.32E−05	59.3	1.44E−09	60	2.63E−08
58.7	1.75E−07	59.4	1.93E−07	60.1	1.7E−06
58.8	3.21E−10	59.5	7.98E−09	60.2	3.85E−07
58.9	1.41E−07	59.6	6.59E−08	60.3	3.5E−07
59	1.37E−07	59.7	4.54E−07	60.4	1.5E−06
59.1	5.54E−08	59.8	3.22E−08	60.5	1.11E−06

Table 2
RMSEs of standard power signal [Eq. (10) and RA].

f (Hz)	RMSE (Hz)	f (Hz)	RMSE (Hz)	f (Hz)	RMSE (Hz)
58.5	1.81E−05	59.2	7.66E−06	59.9	1.86E−07
58.6	3.66E−05	59.3	2.75E−08	60	7.28E−07
58.7	9.13E−09	59.4	8.3E−09	60.1	1.13E−06
58.8	1.24E−06	59.5	8.28E−08	60.2	2.51E−06
58.9	9.69E−07	59.6	9.78E−07	60.3	9.23E−09
59	8.47E−08	59.7	5.88E−10	60.4	5.43E−08
58.5	2.17E−06	59.2	8.06E−07	60.5	7.93E−07

Table 3
RMSEs of standard power signal [Eq. (6) and GA].

f (Hz)	RMSE (Hz)	f (Hz)	RMSE (Hz)	f (Hz)	RMSE (Hz)
58.5	0.000339	59.2	0.001499	59.9	0.000137
58.6	0.000917	59.3	0.000107	60	4.06E−15
58.7	0.001024	59.4	0.0003	60.1	0.000313
58.8	0.00068	59.5	0.000137	60.2	0.000192
58.9	0.000557	59.6	0.000821	60.3	0.000426
59	0.001845	59.7	0.00074	60.4	3.35E−15
59.1	0.000327	59.8	7.54E−06	60.5	1.23E−05

Table 4
RMSEs of standard power signal [Eq. (10) and GA].

f (Hz)	RMSE (Hz)	f (Hz)	RMSE (Hz)	f (Hz)	RMSE (Hz)
58.5	0.001626	59.2	0.00109	59.9	0.000272
58.6	0.001609	59.3	0.001102	60	0.000791
58.7	0.001282	59.4	0.000414	60.1	0.000186
58.8	0.001176	59.5	0.000996	60.2	0.000551
58.9	0.001673	59.6	0.000713	60.3	0.000677
59	0.000954	59.7	0.000714	60.4	0.000451
58.5	0.000922	59.2	0.001153	60.5	0.000617

3.2 Power system signal with harmonics

In this case, the sampling frequency is 960 Hz, the window length is 12 cycles, and the simulation time is 0.2094 s. The following equation is used to represent the input signal:

$$x(t) = \cos\left(2\pi ft + \frac{\pi}{6}\right) + 0.02\cos\left(2\pi fNt + N\frac{\pi}{6}\right),\ N = 3-9, \tag{16}$$

where $x(t)$ is the input signal, f is the fundamental, t is the time, and N is the harmonic order. The frequency range is set to 58.5–60.5 Hz, and the frequency calculation results are shown in Figs. 5 and 6. The RMSEs for both models are shown in Tables 5–8.

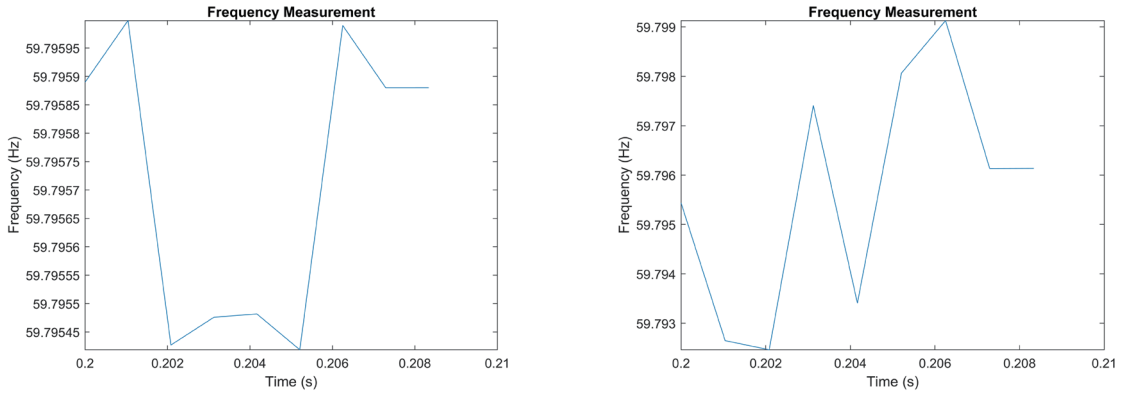

(a) (b)

Fig. 5. (Color online) Frequency 59.8 Hz measurements with 9th harmonic: (a) Eq. (6) and RA, and (b) Eq. (10) and RA.

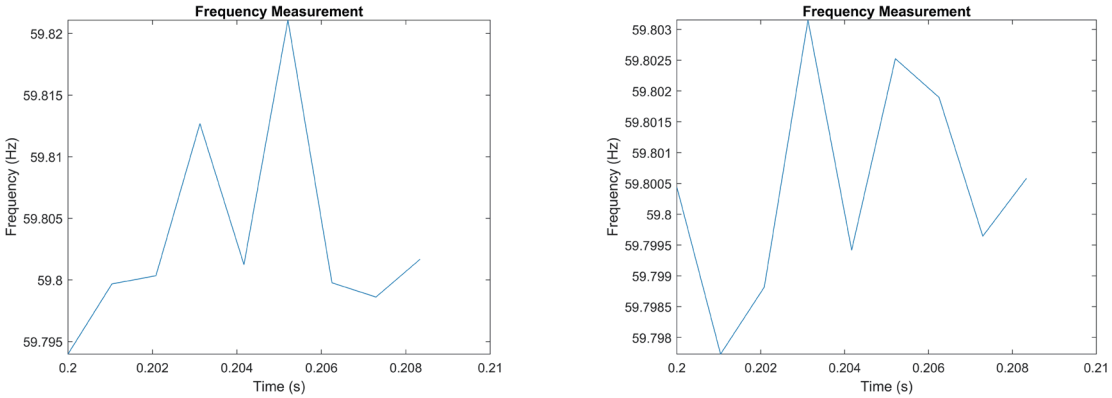

(a) (b)

Fig. 6. (Color online) Frequency 59.8 Hz measurements with 9th harmonic: (a) Eq. (6) and GA, and (b) Eq. (10) and GA.

Table 5
RMSEs of harmonic power signal [Eq. (6) and RA].

f (Hz)	RMSE (Hz)	f (Hz)	RMSE (Hz)	f (Hz)	RMSE (Hz)
58.5	0.000446	59.2	0.000316	59.9	0.002017
58.6	0.00028	59.3	0.000484	60	0.000512
58.7	0.000358	59.4	0.000849	60.1	0.001375
58.8	0.00042	59.5	0.000872	60.2	0.002078
58.9	0.00035	59.6	0.000606	60.3	0.001436
59	0.000483	59.7	0.001495	60.4	0.000927
59.1	0.000612	59.8	0.004291	60.5	0.000613

Table 6
RMSEs of harmonic power signal [Eq. (10) and RA].

f (Hz)	RMSE (Hz)	f (Hz)	RMSE (Hz)	f (Hz)	RMSE (Hz)
58.5	0.001842	59.2	0.002061	59.9	0.003161
58.6	0.001833	59.3	0.006031	60	0.000535
58.7	0.002867	59.4	0.001592	60.1	0.001613
58.8	0.002008	59.5	0.001037	60.2	0.010047
58.9	0.001584	59.6	0.011553	60.3	0.015428
59	0.003304	59.7	0.012033	60.4	0.002479
58.5	0.001789	59.2	0.004901	60.5	0.005144

Table 7
RMSEs of harmonic power signal [Eq. (6) and GA].

f (Hz)	RMSE (Hz)	f (Hz)	RMSE (Hz)	f (Hz)	RMSE (Hz)
58.5	0.003995	59.2	0.003411	59.9	0.006426
58.6	0.004247	59.3	0.006142	60	0.001077
58.7	0.005403	59.4	0.004237	60.1	0.000992
58.8	0.004815	59.5	0.004012	60.2	0.003863
58.9	0.005078	59.6	0.005879	60.3	0.003837
59	0.005349	59.7	0.003722	60.4	0.004494
59.1	0.00286	59.8	0.003304	60.5	0.004229

Table 8
RMSEs of harmonic power signal [Eq. (10) and GA].

f (Hz)	RMSE (Hz)	f (Hz)	RMSE (Hz)	f (Hz)	RMSE (Hz)
58.5	0.00366	59.2	0.004317	59.9	0.001617
58.6	0.002995	59.3	0.003069	60	0.001357
58.7	0.003209	59.4	0.002861	60.1	0.00155
58.8	0.003264	59.5	0.002335	60.2	0.001926
58.9	0.003136	59.6	0.002316	60.3	0.002282
59	0.002786	59.7	0.00244	60.4	0.001957
59.1	0.003174	59.8	0.001992	60.5	0.002203

3.3 Power system signal with harmonics and noises

In this case, the sampling frequency is 960 Hz, the window length is 12 cycles, and the simulation time is 0.2094 s. Equation (17) is used to represent the input signal. White noise of different intensity, i.e., 60–20 dB, is added. The calculation results are shown in Figs. 7–12. The RMSEs are shown in Tables 9–20.

$$x(t) = \cos\left(2\pi ft + \frac{\pi}{6}\right) + 0.02\cos\left(2\pi fNt + N\frac{\pi}{6}\right) + noise(t),\ N = 3-9\,. \tag{17}$$

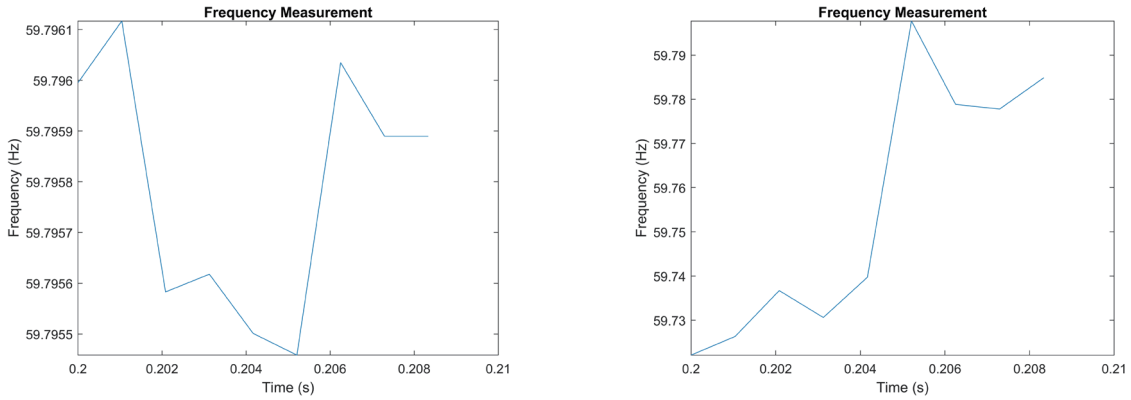

(a) (b)

Fig. 7. (Color online) Frequency 59.8 Hz calculations with 9th harmonic with 60 dB noise: (a) Eq. (6) and RA, and (b) Eq. (10) and RA.

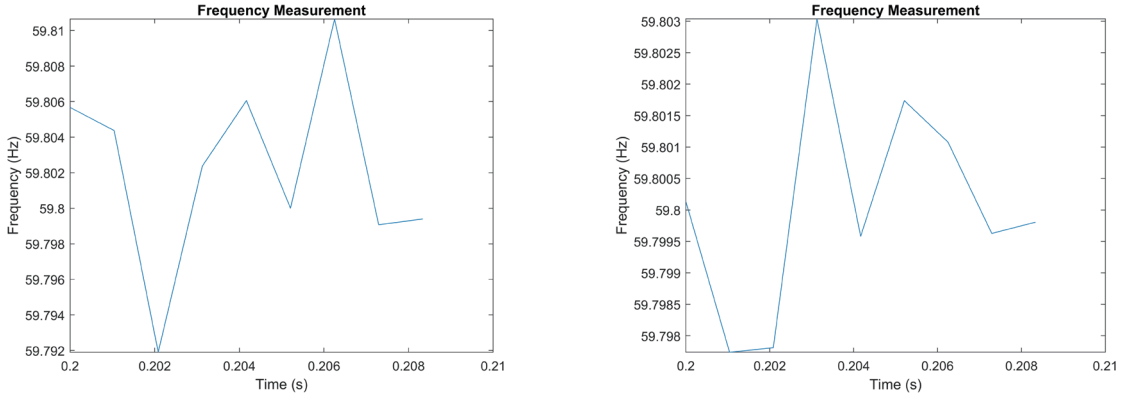

(a) (b)

Fig. 8. (Color online) Frequency 59.8 Hz calculations with 9th harmonic with 60 dB noise: (a)Eq. (6) and GA, and (b) Eq. (10) and GA.

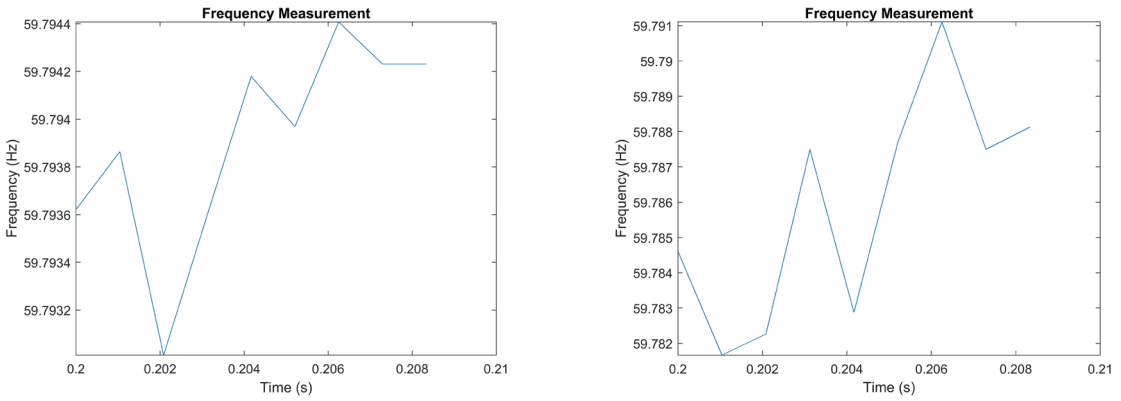

(a) (b)

Fig. 9. (Color online) Frequency 59.8 Hz calculations with 9th harmonic with 40 dB noise: (a) Eq. (6) and RA, and (b) Eq. (10) and RA.

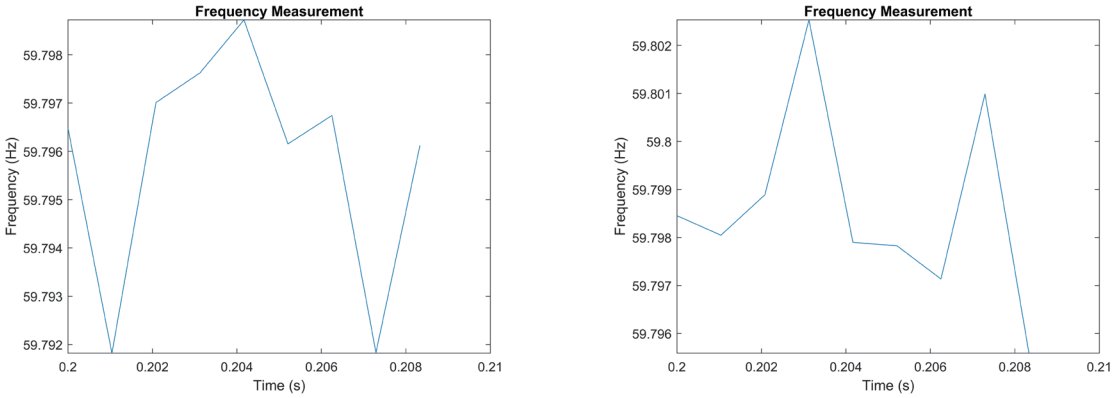

(a) (b)

Fig. 10. (Color online) Frequency 59.8 Hz calculations with 9th harmonic with 40 dB noise: (a) Eq. (6) and GA, and (b) Eq. (10) and GA.

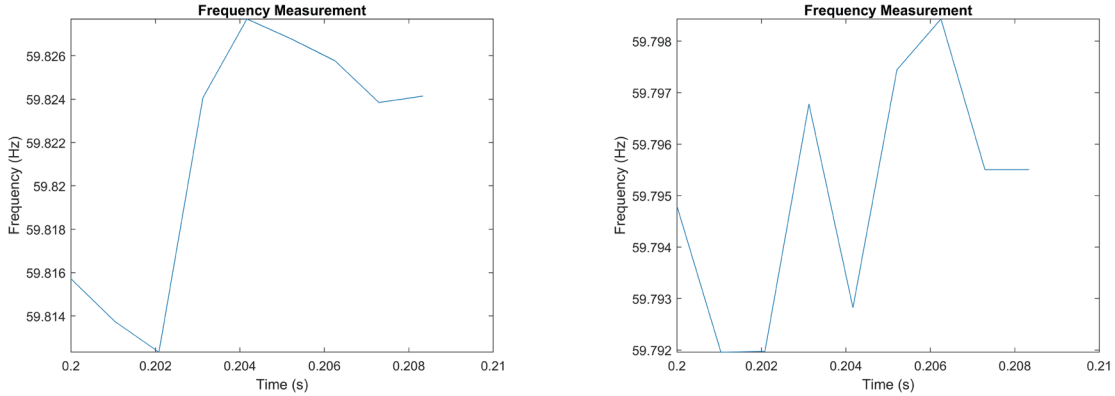

(a) (b)

Fig. 11. (Color online) Frequency 59.8 Hz calculations with 9th harmonic with 20 dB noise: (a) Eq. (6) and RA, and (b) Eq. (10) and RA.

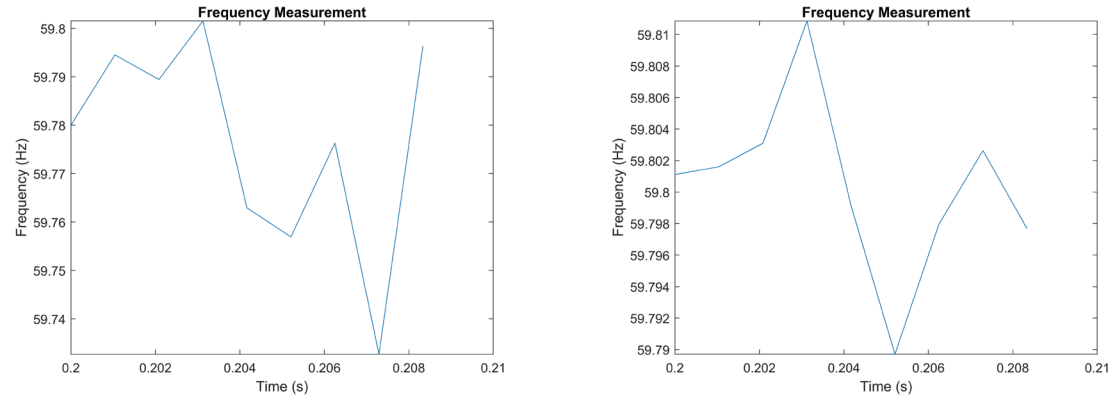

(a) (b)

Fig. 12. (Color online) Frequency 59.8 Hz calculations with 9th harmonic with 20 dB noise: (a) Eq. (6) and GA, and (b) Eq. (10) and GA.

Table 9
RMSEs of harmonic and 60 dB noise power signal [Eq. (6) and RA].

f (Hz)	RMSE (Hz)	f (Hz)	RMSE (Hz)	f (Hz)	RMSE (Hz)
58.5	0.000537	59.2	0.000335	59.9	0.002047
58.6	0.000343	59.3	0.000505	60	0.00051
58.7	0.000412	59.4	0.000918	60.1	0.001349
58.8	0.000465	59.5	0.000836	60.2	0.002061
58.9	0.000413	59.6	0.000597	60.3	0.00148
59	0.000495	59.7	0.001459	60.4	0.000891
59.1	0.000659	59.8	0.0043	60.5	0.000623

Table 10
RMSEs of harmonic and 60 dB noise power signal [Eq. (10) and RA].

f (Hz)	RMSE (Hz)	f (Hz)	RMSE (Hz)	f (Hz)	RMSE (Hz)
58.5	0.001696	59.2	0.00228	59.9	0.003274
58.6	0.002077	59.3	0.006181	60	0.000828
58.7	0.003179	59.4	0.001736	60.1	0.001703
58.8	0.001979	59.5	0.001335	60.2	0.009941
58.9	0.001818	59.6	0.011379	60.3	0.015242
59	0.00288	59.7	0.0123	60.4	0.002682
59.1	0.001944	59.8	0.004681	60.5	0.004716

Table 11
RMSEs of harmonic and 60 dB noise power signal [Eq. (6) and GA].

f (Hz)	RMSE (Hz)	f (Hz)	RMSE (Hz)	f (Hz)	RMSE (Hz)
58.5	0.004305	59.2	0.007171	59.9	0.005738
58.6	0.006607	59.3	0.006405	60	0.00117
58.7	0.005177	59.4	0.006114	60.1	0.000971
58.8	0.005588	59.5	0.003486	60.2	0.003982
58.9	0.005072	59.6	0.003355	60.3	0.00469
59	0.002402	59.7	0.003762	60.4	0.002805
59.1	0.002751	59.8	0.006048	60.5	0.004211

Table 12
RMSEs of harmonic and 60 dB noise power signal [Eq. (10) and GA].

f (Hz)	RMSE (Hz)	f (Hz)	RMSE (Hz)	f (Hz)	RMSE (Hz)
58.5	0.003677	59.2	0.003584	59.9	0.001576
58.6	0.002814	59.3	0.003171	60	0.001223
58.7	0.003426	59.4	0.00244	60.1	0.001248
58.8	0.002595	59.5	0.002436	60.2	0.002484
58.9	0.003067	59.6	0.002377	60.3	0.002209
59	0.002927	59.7	0.00271	60.4	0.002369
59.1	0.002952	59.8	0.002035	60.5	0.002184

Table 13
RMSEs of harmonic and 40 dB noise power signal [Eq. (6) and RA].

f (Hz)	RMSE (Hz)	f (Hz)	RMSE (Hz)	f (Hz)	RMSE (Hz)
58.5	0.001362	59.2	0.001659	59.9	0.002894
58.6	0.001152	59.3	0.002058	60	0.00183
58.7	0.001302	59.4	0.001659	60.1	0.002075
58.8	0.002025	59.5	0.001691	60.2	0.002508
58.9	0.001619	59.6	0.002333	60.3	0.001709
59	0.001497	59.7	0.001699	60.4	0.001742
59.1	0.001385	59.8	0.003089	60.5	0.002415

Table 14
RMSEs of harmonic and 40 dB noise power signal [Eq. (10) and RA].

f (Hz)	RMSE (Hz)	f (Hz)	RMSE (Hz)	f (Hz)	RMSE (Hz)
58.5	0.006214	59.2	0.007832	59.9	0.007874
58.6	0.007982	59.3	0.010755	60	0.006007
58.7	0.008841	59.4	0.005165	60.1	0.009361
58.8	0.007319	59.5	0.008891	60.2	0.008205
58.9	0.008148	59.6	0.011191	60.3	0.013502
59	0.006512	59.7	0.014707	60.4	0.006042
59.1	0.007491	59.8	0.00774	60.5	0.006374

Table 15
RMSEs of harmonic and 40 dB noise power signal [Eq. (6) and GA].

f (Hz)	RMSE (Hz)	f (Hz)	RMSE (Hz)	f (Hz)	RMSE (Hz)
58.5	0.009427	59.2	0.006123	59.9	0.007803
58.6	0.007683	59.3	0.005632	60	0.001728
58.7	0.0071	59.4	0.007734	60.1	0.001093
58.8	0.010812	59.5	0.007417	60.2	0.006873
58.9	0.005827	59.6	0.007574	60.3	0.004832
59	0.008152	59.7	0.007223	60.4	0.006008
59.1	0.006839	59.8	0.007883	60.5	0.006602

Table 16
RMSEs of harmonic and 40 dB noise power signal [Eq. (10) and GA].

f (Hz)	RMSE (Hz)	f (Hz)	RMSE (Hz)	f (Hz)	RMSE (Hz)
58.5	0.003	59.2	0.003554	59.9	0.004313
58.6	0.005708	59.3	0.005499	60	0.00408
58.7	0.004696	59.4	0.00304	60.1	0.002849
58.8	0.004174	59.5	0.003721	60.2	0.004086
58.9	0.002893	59.6	0.004372	60.3	0.003147
59	0.00319	59.7	0.004248	60.4	0.003022
59.1	0.002885	59.8	0.00356	60.5	0.003724

Table 17
RMSEs of harmonic and 20 dB noise power signal [Eq. (6) and RA].

f (Hz)	RMSE (Hz)	f (Hz)	RMSE (Hz)	f (Hz)	RMSE (Hz)
58.5	0.016344	59.2	0.014299	59.9	0.016177
58.6	0.010531	59.3	0.022039	60	0.024712
58.7	0.013036	59.4	0.020986	60.1	0.016582
58.8	0.014342	59.5	0.018493	60.2	0.013603
58.9	0.011518	59.6	0.01435	60.3	0.021486
59	0.016743	59.7	0.019673	60.4	0.017439
59.1	0.015951	59.8	0.022623	60.5	0.019932

Table 18
RMSEs of harmonic and 20 dB noise power signal [Eq. (10) and RA].

f (Hz)	RMSE (Hz)	f (Hz)	RMSE (Hz)	f (Hz)	RMSE (Hz)
58.5	0.085814	59.2	0.058583	59.9	0.053761
58.6	0.045563	59.3	0.065994	60	0.064538
58.7	0.076024	59.4	0.079514	60.1	0.067611
58.8	0.082828	59.5	0.057355	60.2	0.088279
58.9	0.069745	59.6	0.073257	60.3	0.070944
59	0.043449	59.7	0.059322	60.4	0.066609
59.1	0.059615	59.8	0.054493	60.5	0.052876

Table 19
RMSEs of harmonic and 20 dB noise power signal [Eq. (6) and GA].

f (Hz)	RMSE (Hz)	f (Hz)	RMSE (Hz)	f (Hz)	RMSE (Hz)
58.5	0.035569	59.2	0.033859	59.9	0.050711
58.6	0.036338	59.3	0.043532	60	0.026316
58.7	0.043971	59.4	0.037918	60.1	0.046133
58.8	0.030598	59.5	0.044124	60.2	0.045931
58.9	0.033336	59.6	0.041509	60.3	0.041285
59	0.032437	59.7	0.030183	60.4	0.042214
59.1	0.039857	59.8	0.034195	60.5	0.039433

Table 20
RMSEs of harmonic and 20 dB noise power signal [Eq. (10) and GA].

f (Hz)	RMSE (Hz)	f (Hz)	RMSE (Hz)	f (Hz)	RMSE (Hz)
58.5	0.016311	59.2	0.022527	59.9	0.028695
58.6	0.013756	59.3	0.008388	60	0.012257
58.7	0.013646	59.4	0.022163	60.1	0.014579
58.8	0.014095	59.5	0.013848	60.2	0.006766
58.9	0.0243	59.6	0.009921	60.3	0.010077
59	0.006984	59.7	0.006151	60.4	0.009886
59.1	0.020135	59.8	0.014596	60.5	0.021044

3.4 Frequency variation power signal measurement

In this case, the sampling frequency is 960 Hz, the window length is 6 cycles, and the simulation time is 0.25 s. The frequency of the input signal is changed from 60 to 59 Hz at 1 to 1.1 s. The calculation results are shown in Figs. 13 and 14. The RMSEs are shown in Table 21.

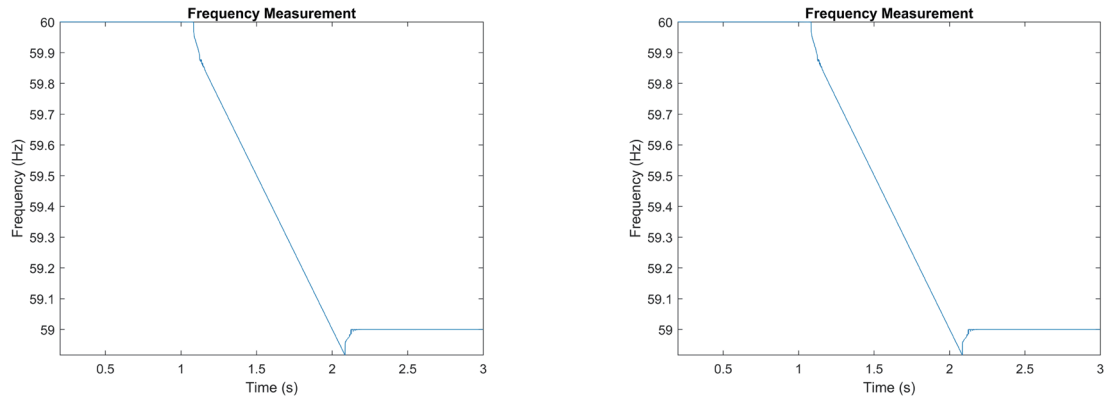

(a) (b)

Fig. 13. (Color online) Frequency changes from 60 to 59 Hz. Frequency calculations obtained using (a) Eq. (6) and RA, and (b) Eq. (10) and RA.

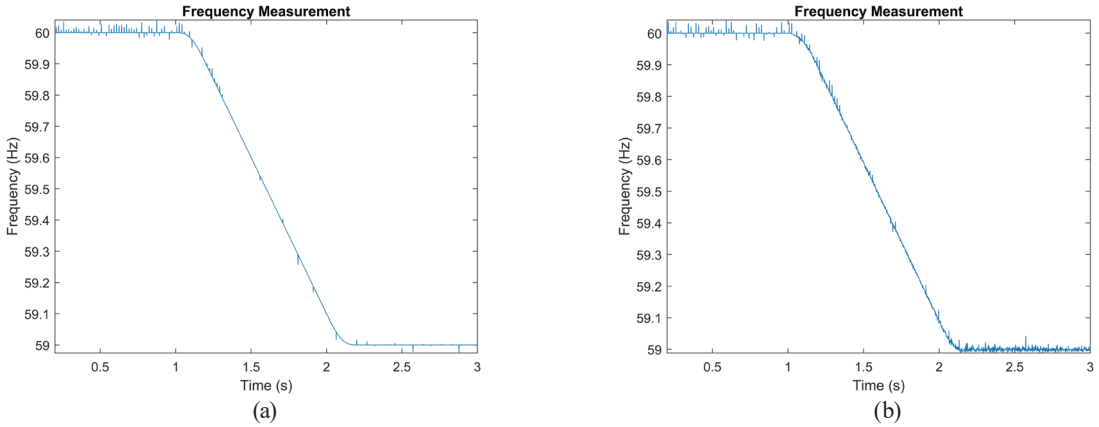

(a) (b)

Fig. 14. (Color online) Frequency changes from 60 to 59 Hz. Frequency calculations obtained using (a) Eq. (6) and GA, and (b) Eq. (10) and GA.

Table 21
RMSEs of RA and GA in frequency modulation.

	RA	GA
Mode	RMSE (Hz)	RMSE (Hz)
Equation (6)	0.1159	0.0574
Equation (10)	0.1159	0.0635

4. Conclusions

In this study, the power system fundamental frequency is calculated using Eqs. (6) and (10). The experimental results in Sect. 3.1 show that the frequency estimation variation of Eq. (6) indicates a smaller RMSE than that of Eq. (10) when the signal is in the steady state. According to the results in Sects. 3.2 and 3.3, the model using Eq. (6) obtains a more accurate frequency estimation than that using Eq. (10) for RA, when signals involve harmonics and noise. In addition, GA is used instead of the conventional RA. It is found from the experimental results that the frequency estimation accuracy using RA decreases when the frequency offset increases. Therefore, RA is not suitable for use in situations where the frequency variation is large. The results of using GA show that the measurement accuracy does not change markedly with the frequency offset. It is found from Sect. 3.4 that when the power signals are used, the RMSE of GA is only half of that of RA, and that the curve is smoother. The overall performance obtained using Eq. (6) is as good or higher than that obtained using Eq. (10) for RA and GA for a steady state. On the other hand, GA performs better than RA in terms of frequency tracking. From the obtained results, it is found that Eqs. (6) and (10) are not perfect mathematical models to represent the frequency variation of power systems. These equations can be further improved to handle more complex signals, e.g., flicker. In the future, it may be necessary to design a model and a more accurate parametric learning algorithm that can better match a waveform under frequency variation so that the residual can be lower and the accuracy of the frequency estimation can be further improved.

Acknowledgments

This study was partially supported in part by the Ministry of Science and Technology, Taiwan, under Grant Nos. MOST 106-2221-E-027-086-MY2 and MOST 107-3114-F-492-001- and MOST 108-3116-F-006-008-CC2 and the “Research Center of Energy Conservation for New Generation of Residential, Commercial, and Industrial Sectors” from The Featured Areas Research Center Program within the framework of the Higher Education Sprout Project by the Ministry of Education (MOE) in Taiwan.

References

1 J. Ren and M. Kezunovic: IEEE Trans. Power Delivery **27** (2012) 1252. https://doi.org/10.1109/tpwrd.2012.2196770

2 M. S. Reza, M. Ciobotaru, and V. G. Agelidis: IEEE Trans. Instrum. Meas. **64** (2015) 615. https://doi.org/10.1109/tim.2014.2347671
3 S.-R. Nam, S.-H. Kang, and S.-H. Kang: Energies **8** (2014) 79. https://doi.org/10.3390/en8010079
4 H. Xue, M. Wang, R. Yang, and Y. Zhang: IEEE Trans. Instrum. Meas. **65** (2016) 56. https://doi.org/10.1109/tim.2015.2477157
5 D. Camarena-Martinez, M. Valtierra-Rodriguez, C. A. Perez-Ramirez, J. P. Amezquita-Sanchez, R. de Jesus Romero-Troncoso, and A. Garcia-Perez: IEEE Trans. Ind. Electron. **63** (2016) 2369. https://doi.org/10.1109/tie.2015.2506619
6 C.-H. Lee and M.-S. Tsai: Meas. Sci. Technol. **29** (2018) 065001. https://doi.org/10.1088/1361-6501/aab943
7 T. Lobos and J. Rezmer: IEEE Trans. Instrum. Meas. **46** (1997) 877. https://doi.org/10.1109/19.650792
8 J. A. de la O Serna: IEEE Trans. Instrum. Meas. **62** (2013) 2119. https://doi.org/10.1109/tim.2013.2265436
9 M. B. Djurić and Ž. R. Djurišić: Electr. Power Syst. Res. **78** (2008) 1407. https://doi.org/10.1016/j.epsr.2008.01.008
10 Y.-C. Chen and T.-H. Chien: Appl. Math. Inform. Sci. **9** (2015) 65. https://doi.org/10.12785/amis/091L08
11 IEEE Std 1459-**2000** (2000) 1. https://doi.org/10.1109/IEEESTD.2000.93398
12 H. Kirkham and A. Riepnieks: 2016 57th Int. Scientific Conf. Power and Electrical Engineering of Riga Technical University (RTUCON, 2016) 1. https://doi.org/10.1109/RTUCON.2016.7763125
13 IEEE Std C37.118.2-2011 (Revision of IEEE Std C37.118-2005) (2011) 1. https://doi.org/10.1109/IEEESTD.2011.6111222
14 H. Kirkham and A. Riepnieks: 2016 IEEE Power and Energy Society General Meeting (PESGM, 2016) 1. https://doi.org/10.1109/PESGM.2016.7741270
15 M. A. Rodriguez-Guerrero, R. Carranza-Lopez-Padilla, R. A. Osornio-Rios, and R. de J. Romero-Troncoso: Elect. Power Syst. Res. **143** (2017) 14. https://doi.org/10.1016/j.epsr.2016.09.003
16 K. F. Man, K. S. Tang, and S. Kwong: IEEE Trans. Industr. Electron. **43** (1996) 519. https://doi.org/10.1109/41.538609
17 S. J. Ovaska, A. Kamiya, and C. YangQuan: IEEE Trans. Syst. Man Cybern. Part C App. Rev. **36** (2006) 439. https://doi.org/10.1109/tsmcc.2005.855528
18 C. J. Gabbe: Sustainable Cities Soc. **42** (2018) 611. https://doi.org/10.1016/j.scs.2018.07.020
19 Y. Guo, K. Li, D. M. Laverty, and Y. Xue: IEEE Trans. Power Delivery **30** (2015) 2544. https://doi.org/10.1109/tpwrd.2015.2435158
20 A. Rav, K. D. Joshi, K. Roy, and T. C. Kaushik: Meas. Sci. Technol. **28** (2017) 055202. https://doi.org/10.1088/1361-6501/aa5d49

About the Authors

Chih-Hung Lee was born in Taiwan, on April 8, 1986. He received his MS degree from the Graduate Institute of Automation Technology, National Taipei University of Technology in 2011. He is currently a Ph.D. student of the Graduate Institute of Mechanical and Electrical Engineering, National Taipei University of Technology, Taipei, Taiwan. His research areas include the signal processing of power quality measurements.
(t100669021@ntut.edu.tw)

Chi-Chun Huang received his B.S. degree in mechanical engineering from Chung Yuan Christian University, Taiwan, in 2012. He is an M.S. student of the National Taipei University of Technology, Taiwan. His research interest is in power systems. (t106618017@ntut.edu.tw)

Men-Shen Tsai (M'86) was born in Taiwan in 1961. He received his Ph.D. degree from the Department of Electrical Engineering, University of Washington, Seattle, in 1993. He is currently a professor of the Graduate Institute of Automation Technology, National Taipei University of Technology, Taipei, Taiwan. His research areas include applications of intelligent systems to power systems and applications of distributed technologies for distribution automation. (mstsai@ntut.edu.tw)